American College of Neuropsychopharmacology

www.nature.com/npp

ARTICLE

Check for updates

Pharmacogenetic activation of parvalbumin interneurons in the prefrontal cortex rescues cognitive deficits induced by adolescent MK801 administration

Linda A. Chamberlin[1,2], Sha-Sha Yang[1,3], Erin P. McEachern[1], Joshua T. M. Lucas[4], Owen W. McLeod II[5], Claire A. Rolland[5], Nancy R. Mack[1], Brielle R. Ferguson[1,6]✉ and Wen-Jun Gao[1]✉

© The Author(s), under exclusive licence to American College of Neuropsychopharmacology 2023

The cognitive symptoms of schizophrenia (SZ) present a significant clinical burden. They are treatment resistant and are the primary predictor of functional outcomes. Although the neural mechanisms underlying these deficits remain unclear, pathological GABAergic signaling likely plays an essential role. Perturbations with parvalbumin (PV)-expressing fast-spiking (FS) interneurons in the prefrontal cortex (PFC) are consistently found in post-mortem studies of patients with SZ, as well as in animal models. Our studies have shown decreased prefrontal synaptic inhibition and PV immunostaining, along with working memory and cognitive flexibility deficits in the MK801 model. To test the hypothesized association between PV cell perturbations and impaired cognition in SZ, we activated prefrontal PV cells by using an excitatory DREADD viral vector with a PV promoter to rescue the cognitive deficits induced by adolescent MK801 administration in female rats. We found that targeted pharmacogenetic upregulation of prefrontal PV interneuron activity can restore E/I balance and improve cognition in the MK801 model. Our findings support the hypothesis that the reduced PV cell activity levels disrupt GABA transmission, resulting in the disinhibition of excitatory pyramidal cells. This disinhibition leads to an elevated prefrontal excitation/inhibition (E/I) balance that could be causal for cognitive impairments. Our study provides novel insights into the causal role of PV cells in cognitive function and has clinical implications for understanding the pathophysiology and management of SZ.

Neuropsychopharmacology (2023) 48:1267–1276; https://doi.org/10.1038/s41386-023-01576-6

INTRODUCTION

Cognitive symptoms in schizophrenia (SZ) are unresponsive to treatment with either typical or atypical antipsychotics [1–4]. Therefore, the development of treatments for cognitive deficits represents a critical subject for research. A strong candidate in the underlying pathophysiology of cognitive deficits in SZ is GABAergic neurotransmission. Downregulation of the metabolic enzyme that synthesizes GABA, glutamate decarboxylase-67, is the most commonly observed alteration in SZ post-mortem tissue [5–10]. This decrease occurs specifically in parvalbumin (PV)-positive interneurons, whose function is linked to gamma oscillations and cognition [11, 12]. Pathological inhibitory transmission is also a point of convergence across a myriad of preclinical SZ models. Decreased PV, a protein with activity-dependent expression, has been reported in various animal models for SZ, including the neonatal ventral hippocampal lesion, methylazoxymethanol acetate, NMDAR receptor antagonism (PCP, ketamine, and MK801), and transgenic models (such as dysbindin and neuregulin 1) [13–22]. However, it remains unknown whether GABAergic pathology is a primary cause of the disorder or is just intimately associated with the ultimate disease processes.

Our recent studies have provided rigorous evidence of decreased GABAergic signaling as well as cognitive deficits, such as impaired working memory and learning in MK801-treated animals [23–26]. Specifically, MK801 administration during adolescence significantly reduces the activity of PV-expressing FS interneurons in the medial prefrontal cortex (mPFC) and induces enduring SZ-like symptoms [24, 26–28]. However, while the reduction of PV is closely correlated with cognitive deficits, it remains elusive whether increasing the activity of prefrontal PV neurons is sufficient to reverse the cognitive deficits.

Here, we use a novel excitatory designer receptor exclusively activated by designer drugs (DREADD) driven by a PV promoter to directly increase GABAergic signaling. Specifically, we explored whether pharmacogenetic enhancement of PFC PV interneuron activity could improve cognitive performance in female rats, directly confirming our hypothesis. We found that targeted pharmacogenetic upregulation of prefrontal PV interneuron activity can restore E/I balance and improve cognition in the MK801 model. Our study provides novel insights into the causal role of PV cells in cognitive function and has clinical implications for understanding the pathophysiology and treatment of SZ.

[1]Department of Neurobiology & Anatomy, Drexel University College of Medicine, Philadelphia, PA, USA. [2]MD/PhD program, Drexel University College of Medicine, Philadelphia, PA, USA. [3]Institute for Translational Brain Research, Department of Neurology, Fudan University, Shanghai 200032, China. [4]MD program, Drexel University College of Medicine, Philadelphia, PA, USA. [5]Interdisciplinary Health Sciences Program, Drexel University College of Medicine, Philadelphia, PA, USA. [6]2 Blackfan circle, Cetern for Life Science, Boston, MA 02115, USA. ✉email: Brielle_Ferguson@hms.harvard.edu; wg38@drexel.edu

Received: 26 June 2022 Revised: 23 March 2023 Accepted: 26 March 2023
Published online: 11 April 2023

MATERIALS AND METHODS

Animals

Many pharmacological studies indicate that female rats are more sensitive to MK801 than male rats [29–31]. Also, to be consistent with our previous studies [24–26], adolescent female rats were treated with either MK801 (0.1 mg/kg, Tocris Bioscience, Minneapolis, MN, USA) or a volume-matched injection of saline as a control, intraperitoneally (i.p.), daily for 5 consecutive days (postnatal day 40 to 44: P40-44) [26]. All procedures involving animals were approved by the Institutional Animal Care and Use Committee of Drexel University and conducted in accordance with the National Institute of Health guidelines. Detailed experimental procedures can be found in the flowchart of Fig. 1 and Supplementary Information.

Viral vectors

A custom-made adeno-associated virus (AAV) was purchased from the University of North Carolina Vector Core Facility (Chapel Hill, NC, USA), wherein the hM3Dq DREADD receptor was inserted into the AAV8-fPV-GFP vector [32], as reported in our recent study (Fig. 5A–C and Supplementary Information for details) [33]. Given that CaMKIIα is selectively expressed in cortical pyramidal neurons but not GABAergic interneurons [34], AAV8-CaMKIIalpha-eGFP was purchased from Addgene (Watertown, MA, USA) as a control virus. All viral vectors were stored in aliquots at −80 °C until use. Animals were divided into four groups (see Supplementary Table 1): Control (saline-saline or saline with control virus with or without Clozapine-N-Oxide/CNO or PV-DREADD virus without CNO), MK801 (MK801 with control virus with or without CNO or PV-DREADD virus without CNO), Rescue (MK801 injection with PV-DREADD virus with CNO), and PV-DREADD (saline injection with PV-DREADD with CNO).

Stereotaxic surgery

Rats received a bilateral viral injection into the mPFC using an ASI Instruments Stereotaxic Frame (ASI Instruments, Warren, MI, USA). The mPFC was defined based on the Rat Brain in Stereotaxic Coordinates by Paxinos and Watson, 6th edition [35]. Briefly, a cannula was slowly lowered to the target coordinates, and the virus was infused at a rate of 9.6 microliters/hour. The cannula remained in place for 5 min post-injection. The final volume was 0.8 µl per side. After surgery, animals recovered for a minimum of 2 weeks.

The four major experimental groups result from adolescent administration of MK801 or saline, and the presence or absence of an activated PV-DREADD (see Supplementary Table 1). Control groups were pooled to increase statistical power as there were no statistical differences among them.

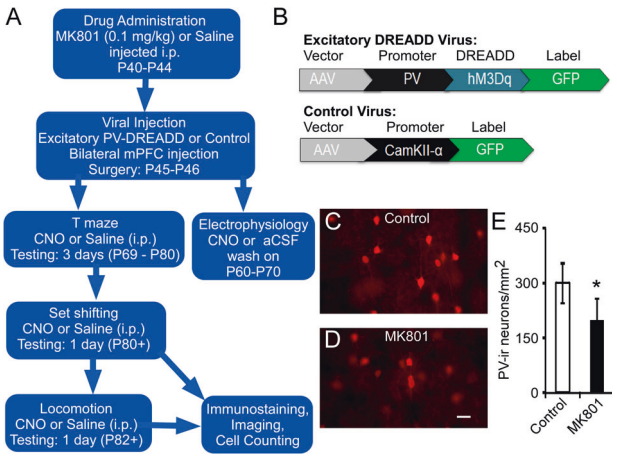


Fig. 1 Experimental Design and PV expression in MK801 mice. **A** Experimental flow chart. All animals received subchronic injections of either saline or MK801 during adolescence and an intracranial injection of either the PV-DREADD virus or the control virus. After allowing time for viral expression, animals used for behavioral experiments started with T-maze. Most of these animals then went on to complete the set-shifting task. A sampling of animals from each experimental group then performed the locomotion task. Following behavioral experiments, histological analysis was performed. Animals who did not undergo behavioral tasks were used for electrophysiological studies. **B** Viral Constructs. Top: The excitatory hM3Dq DREADD is packaged in an AAV, is expressed under control of the PV promoter, and is tagged with GFP for visualization. Bottom: The control virus is also an AAV and tagged with GFP, but there is no DREADD and its expression is under control of the CamKII-α promoter. **C**–**E** Adolescent MK801 administration significantly decreased PV expression in adult rat mPFC. **C**, **D**, Immunostaining of PV in the mPFC of saline control (**C**) and MK801-treated (**D**) animals (Scale bar = 20 µM). **E** MK801 significantly decreased PV-immunoreactive neurons ($n = 5$ each, $p < 0.05$).

Histology & immunohistochemistry

Rats were anesthetized and transcardially perfused, then brains were removed and cryoprotected. Using a microtome, 30 µm sections containing the mPFC were collected. Sections were incubated with an antibody against PV, followed by a red fluorescent secondary antibody. Sections were mounted and coverslipped. Images were acquired with a confocal microscope using a 20x oil immersion objective.

Cell counting

Images collected from confocal microscopy were analyzed using the NIH ImageJ software to assess the distribution of PV neurons and PV expression levels in the PL and IL cortex of rats used in behavioral experiments, as well as to confirm viral expression and specificity of co-expression with PV. Cy5 labeled cells falling within the boundaries of the IL and PL were counted, and fluorescent intensity and distance from the midline were quantified. The density of immunostained neurons was calculated by normalizing to the area of the defined region of interest [36, 37].

Electrophysiology

Rats were anesthetized and perfused with ice-cold artificial cerebrospinal fluid (aCSF) solution. Coronal slices (300 µm) containing the mPFC were collected in ice-cold oxygenated aCSF using a vibratome. Slices were transferred to oxygenated N-methyl-D-glucamine (NMDG) solution that bubbled continuously with 95% O_2 and 5% CO_2, and incubated at 37 °C for 15 min. Slices were then transferred to room temperature oxygenated aCSF for 1 h. Slices were placed into a recording chamber mounted on an upright microscope and bathed in oxygenated aCSF at 37 °C. Neurons were visualized with fluorescent or differential interference contrast (DIC) video microscopy.

To measure the effect of increasing GFP-labeled PV cell activity on the parameter of interest, we recorded cells with or without CNO(5 µM). This was used to activate the $hM3D_q$ receptors expressed by prefrontal PV cells, with the goal of increasing the probability of local, spontaneous release of GABA from these cells. In animals expressing the PV-DREADD-GFP virus, fluorescent labeling also helped with PV cell identification. We recorded from GFP-labeled PV interneurons and pyramidal cells in both layer II/III and layer V of the PL portion of the mPFC.

To confirm the efficacy of the PV-DREADD virus, the frequency of spontaneous inhibitory postsynaptic currents (sIPSCs) was recorded from pyramidal cells with and without CNO present in the bath. These cells were first recorded with NMDA receptor antagonist CPP (10 µM) and voltage clamped at 0 mV, the reversal potential of AMPA receptor-mediated currents. This recording was then repeated with CNO (5 µM) added to the bath. A higher sIPSC frequency in the presence of CNO would reflect the increased activity of inhibitory cells expressing the DREADD.

To record spontaneous excitatory postsynaptic currents (sEPSCs), cells were recorded in the presence of CPP (10 µM) and voltage clamped at −60 mV. Next, sIPSCs were recorded as described above, with CPP and voltage clamped at 0 mV. For spontaneous currents, primary output measures were frequency, amplitude, and decay. The excitation to inhibition (E/I) ratio for each cell was determined by comparing the frequency of the sEPSC and sIPSC recorded from that cell (sEPSC frequency/sIPSC frequency).

Behavior

T-maze. The apparatus was a wooden plus maze (composed of 4 arms each measuring 14.5 × 4.5 × 9.0 inches) with slots at the entry of each arm, allowing for the blockade of individual arms with opaque plexiglass inserts, and food wells at the end of each arm. The north arm was consistently blocked off to create a "T" configuration. Training began with 2 days of habituation. Days 3 and 4 consisted of forced-alteration training. On Day 5, delayed-response training began, in which trials consisted of forced and

free run pairs. Rats were placed in the start arm, and only allowed access to the right arm, for example. Then, the animal was placed in a holding cage for a 10 s (s) delay, then returned to the start arm and given the choice to go either left or right. A choice of the left arm was scored as a correct trial. Following a 40 s intertrial delay, the next trial would begin. To move on to the testing phase, a rat had to reach a criterion of 7 out of 10 correct responses on 3 consecutive days. Testing was identical to the training except that the delay varied between 5, 15, 30, and 60 s. Animals were injected i.p. 45 min prior to the T-maze session on each of the 3 testing days with CNO (5 mg/kg), or an equivalent volume of physiological saline. Groups were compared on days to acquisition, and percentage of correct trials at each delay interval.

Set-shifting task. Following the T-maze, the set-shifting task was carried out [33, 38, 39]. On the first day, animals were habituated to the set-shifting apparatus and trained to dig in bowls that varied in either scent (garlic or coriander) or digging medium (sand or bedding). Animals were injected i.p. 45 min prior to the set-shifting session on the second day with CNO (5 mg/kg), or an equivalent volume of physiological saline. For this day of set-shifting, animals learned that a particular scent predicted the location of the food reward, regardless of the digging medium (initial association). Once the animal met criteria for learning this rule (8 consecutive correct trials), they were presented with a rule shift, so that a digging medium rather than an odor indicated the rewarded bowl. Once the criterion was met for this rule shift, animals were presented with a reversal of the previously rewarded association, so that the other digging medium now predicted the reward location.

Data analysis and statistics

To analyze spontaneous EPSC or IPSC events, a typical current sample was selected to create a template, and EPSC or IPSC events within a 5-min recording period were detected by the Clampfit software. The EPSC or IPSC frequency (number of events) was normalized to events per second (Hz) and the amplitude was measured from the onset to peak of the average trace.

Electrophysiological, behavioral, and histological data were analyzed using SPSS Statistics. All bar graphs are presented as mean ± SEM. Normality was determined using the Shapiro–Wilk test to direct the use of parametric versus non-parametric tests. For normally distributed data, comparison of two independent groups was done using a Student's *t*-test, while paired samples were compared using paired *t*-tests. For data without a normal distribution, a Mann–Whitney *U* test (independent) or Wilcoxon Signed Rank test (paired) was used. For comparisons of multiple groups, a repeated measures ANOVA was used followed by post-hoc Dunnett's test, or Tukey's test for multiple comparisons. $P < 0.05$ was considered significant and was represented by a one asterisk (*), while $p < 0.01$ was represented with two (**), $p < 0.001$ was represented with three (***), and $p < 0.0005$ shown with four (****).

RESULTS

Adolescent administration of MK801 significantly reduced PV expression in the mPFC

A well-replicated finding in postmortem studies of SZ patients and animal models of this disease is a reduction in prefrontal PV, a protein whose expression level increases with PV cell firing. MK801 administration during adolescence significantly reduces the activity of PV-expressing FS interneurons in the mPFC and induces enduring SZ-like symptoms [26, 40]. Our recent studies have provided rigorous evidence of decreased GABAergic signaling as well as cognitive deficits, such as impaired working memory and learning, in MK801-treated animals [23–26]. We first replicated this finding by immunostaining PV cells in the mPFC. As shown in Fig. 1, we found that the density of PV expressing neurons reaching the threshold of visibility was significantly reduced by the administration of MK801.

The PV-DREADD construct is effective in targeting PV cells and increasing postsynaptic inhibition

To increase the activity of prefrontal PV cells, we used a viral vector to deliver an excitatory hM3Dq DREADD construct driven by a PV promoter and tagged with a GFP label [32]. After allowing at least 2 weeks for viral expression, robust GFP labeling was observed in the PL mPFC (Fig. 2A–C). Previous work in our lab has quantified the colocalization of the DREADD with PV expression, and found that 82% of antibody-labeled PV cells were also positive for the hM3Dq DREADD, and 70% of hM3Dq-labeled neurons exhibited a fast-spiking firing [33]. Our findings of robust colocalization echo these data. Also, in keeping with our lab's previous findings, a majority of hM3Dq-labeled neurons demonstrated a fast-spiking phenotype, and those that did not were excluded from analysis. The functionality of the excitatory PV-DREADD was confirmed in slice by bath application of CNO, which resulted in a significant increase in sIPSC frequency recorded from pyramidal cells in the PFC (paired samples *t*-test, $p = 0.012$; Fig. 2D, E).

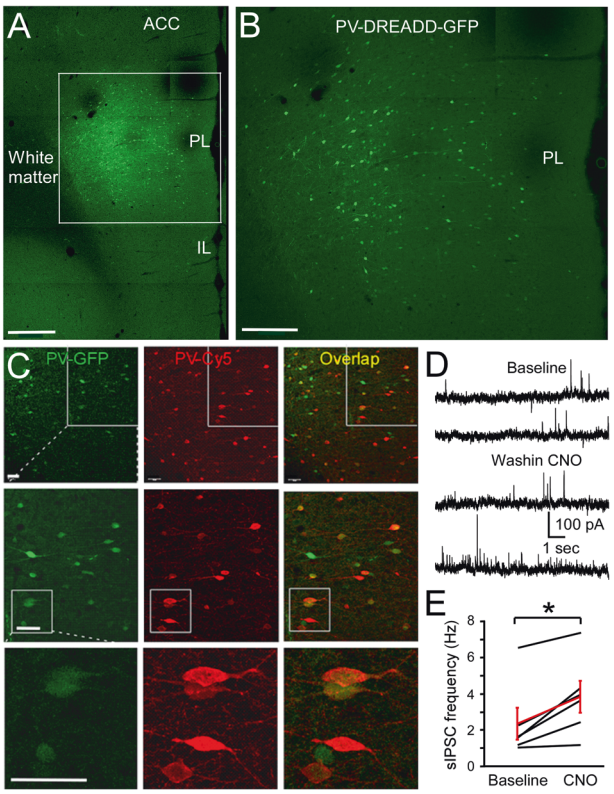
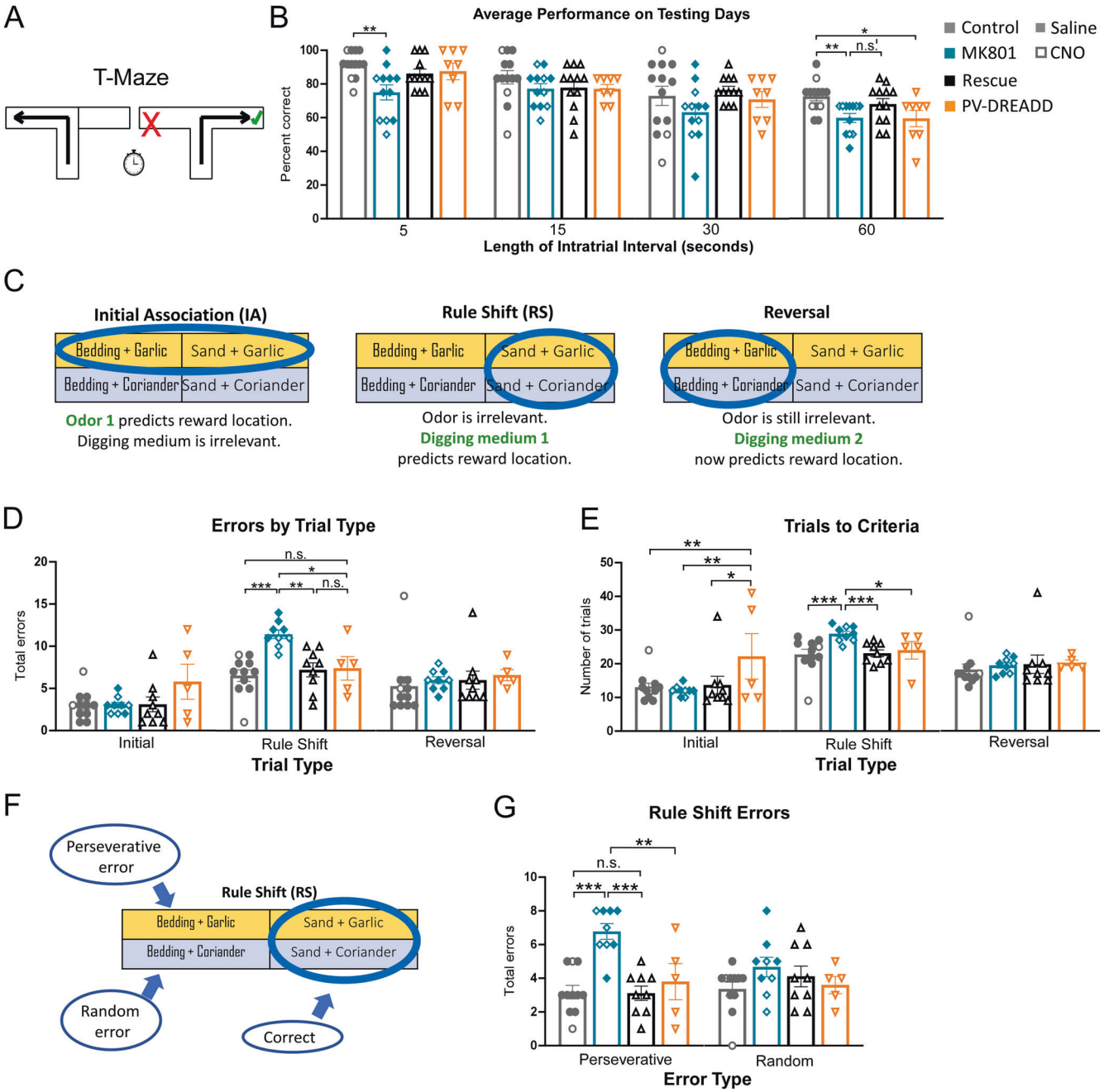


Fig. 2 PV-DREADD Validation. A Injection site of PV-DREADD in the PL of the mPFC. **B** higher magnification of the box in **A**. **C** Photomicrographs showing the GFP fluorescent tag virally expressed with PV-DREADD (left), Cy5-labeled cells targeted with anti-PV immunohistochemistry (middle), and the colocalization of these signals (right). Each image is a magnified view of the white box contained in the image above it. Scale bars: 500, 250, and 50 µm in **A**–**C**, respectively. **D** Sample sIPSC traces from a pyramidal cell in the PFC of an animal with PV-DREADD expression before (above) and after (below) washing on CNO. **E** Adding CNO to the bath elicited a statistically significant increase in sIPSC frequency in pyramidal cells of rats expressing the excitatory PV-DREADD, $n = 6$, $t(5) = 3.867$, $p = 0.012$). Red line: Average change in sIPSC frequency.

Prefrontal PV-DREADD activation ameliorates impairments in spatial working memory and cognitive flexibility in the MK801 model

Because working memory deficits have been well-established in the rodent MK801 model, we used this aspect of cognition to probe the capacity of our prefrontal excitatory PV-DREADD approach to improve performance on a delayed non-match to sample paradigm [23–26]. For this task, rats were trained to alternate entry into the left and right arms of a T-maze to receive a food reward (Fig. 3A).



Performance of MK801-treated rats was significantly worse than that of Control animals ($p = 0.015$), while the Rescue group was not significantly different from the Controls ($p = 1.000$). Performance in the PV-DREADD group fell in between, and was not significantly different from any other group (Fig. 3B). When comparing performance at the different time delays, we see that the greatest difference between Control and MK801 group exists in the 5-s delay trials ($p = 0.006$, Fig. 3B), and again, the Rescue group's performance was not significantly different from that of Controls ($p = 0.644$). No significant group differences exist for the 15- or 30-s delay trials (15 s: $p = 0.924$; 30 s: $p = 0.230$), but group differences emerge again at the 60-s time point. At this longer delay, MK801-treated rats performed significantly worse than Controls ($p = 0.025$), and the Rescue group was not significantly different from Controls ($p = 0.716$). The only time point where excess inhibition caused a significant difference was also at these 60-s delay trials, where PV-DREADD group performed worse than Control animals ($p = 0.047$). Together, these results offer support for a potential role for prefrontal PV cells as a target for restoring disrupted working memory in SZ, especially at the longest and shortest of delay periods.

Animals were not administered CNO until testing, so all MK801-treated animals are pooled, and all saline-treated animals are pooled when assessing days to criterion for the T-maze task. No differences were found between MK801-treated and saline-treated animals in the number of days needed to acquire the task ($p = 0.590$, Supplementary Fig. S1A). There are also no significant differences among the groups in distance traveled during the locomotion task ($p > 0.05$, Fig. S1B–E).

To test cognitive flexibility, animals were trained to dig in sets of bowls that differ in scent and digging medium. Animals must first learn an initial association where a particular scent predicts the

Fig. 3 Prefrontal PV-DREADD activation ameliorates impairments in spatial working memory and cognitive flexibility associated with adolescent MK801 treatment - T-maze. A The T-Maze variable delay non-match to sample test of working memory. **B** Average Performance on Testing Days. A two-way mixed ANOVA showed no statistically significant interaction between the group and delay times, $F(9, 123) = 1.204$, $p = 0.299$, partial eta squared = 0.081. There was a significant difference in performance between groups at the 5-s. delay point, $F(3, 41) = 4.397$, $p = 0.009$, partial eta squared = 0.243. For this brief delay, the Saline group performed better than the MK801-treated animals ($p = 0.006$), but did not differ from the Rescue group ($p = 0.644$). There was no significant difference in performance between groups at the 15-s. delay point, $F(3, 41) = 0.924$, $p = 0.924$, partial eta squared = 0.063. The 30-s delay also showed no significant difference in performance between groups, $F(3, 41) = 1.495$, $p = 0.230$, partial eta squared = 0.099. There was a significant difference in performance between groups at the 60-s. delay point, $F(3, 41) = 4.026$, $p = 0.013$, partial eta squared = 0.228. For this longer delay, saline-treated animals did better than MK801-treated rats ($p = 0.025$) and the PV-DREADD group ($p = 0.047$). The Saline group did not differ significantly from the Rescue group ($p = 0.716$). Note, CNO controls in Saline and MK801 groups were labeled with open symbols in **B**, **D**, **E**, and **G**. **C–G** Prefrontal PV-DREADD activation rescues cognitive flexibility deficits seen in the MK801 model - Set Shifting. **C** Left: The initial association requires the rat to associate an odor with the location of a food reward, regardless of the digging medium. Middle: The EDS requires that the digging medium be attended to in order to receive a reward, while the odor is no longer relevant. Right: The rule reversal asks the animal to associate the previously unrewarded digging medium with the reward. **D** Errors by trial type. A two-way mixed ANOVA showed no significant interaction between group and trial type for number of errors made, $F(4.566, 45.660) = 2.404$, $p = 0.056$, partial eta squared = 0.194, epsilon = 0.761. There was no significant difference in number of errors made between groups for the initial association, $F(3, 30) = 1.840$, $p = 0.161$, partial eta squared = 0.155. There was a significant difference in number of errors made between groups for the rule shift, $F(3, 30) = 8.551$, $p < 0.0005$, partial eta squared = 0.461. Saline-treated rats did better than the MK801 group ($p < 0.0005$) but did not differ from the Rescue group ($p = 0.914$). The MK801 group made more errors in learning the rule shift compared to both the Rescue group ($p = 0.003$) and the PV-DREADD group ($p = 0.019$). **E** Trials to Criteria. A two-way mixed ANOVA showed that there was a significant interaction between group and trial type on trials to criteria, $F(4.379, 93.424) = 4.465$, $p = 0.002$, partial $\eta 2 = 0.173$, $\varepsilon = 0.730$. There was a significant difference in average number of trials to reach criterion between groups for the Initial Association, $F(3, 64) = 5.120$, $p = 0.003$, partial eta squared = 0.194. The PV-DREADD group required more trials than Controls ($p = 0.006$), the MK801 group ($p = 0.003$), and the Rescue group ($p = 0.016$). There was also a significant difference in trials to criterion between groups for acquiring the Rule Shift, $F(3, 64) = 9.229$, $p < 0.0005$, partial eta squared = 0.302. The Control group required substantially fewer trials than the MK801 group ($p < 0.0005$), as did the Rescue group ($p < 0.0005$) and the PV-DREADD group ($p = 0.016$). Also notable is the lack of difference between the Rescue and Control groups. There was no significant difference in trials to criterion between groups for the rule reversal, $F(3, 64) = 0.469$, $p = 0.705$, partial eta squared = 0.021. **F** Two types of error can be made on rule shift trials. **G** Rule Shift Errors. A two-way mixed ANOVA showed a significant interaction between group and error type for number of errors made, $F(3, 30) = 3.714$, $p = 0.022$, partial eta squared = 0.271. There was a significant difference in number of errors made between groups for perseverative errors, $F(3, 30) = 12.003$, $p < 0.0005$, partial eta squared = 0.546. The MK801 group made more perseverative errors than the Control group ($p < 0.0005$), the Rescue group ($p < 0.0005$), and the PV-DREADD group ($p = 0.001$). The Control and Rescue groups did not significantly differ ($p = 0.918$). There was no significant difference in number of errors made between groups for random errors, $F(3, 30) = 1.239$, $p = 0.313$, partial eta squared = 0.110.

location of a food reward (Fig. 3C left). Then there is an extradimensional rule shift (EDS), and the digging medium now predicts the correct choice regardless of the scent (Fig. 3C middle). The final phase is a rule reversal, wherein the previously rewarded and unrewarded media are swapped (Fig. 3C right). Animals are compared on trials to criterion and total errors for acquisition of each rule, and error types (perseverative versus random) for the EDS (Fig. 3C–G). There was no difference in the number of errors each group made as they acquired the initial association on the set-shifting task ($p = 0.161$, Fig. 3D). However, in the EDS, rats in the SZ group showed poor performance ($p < 0.001$, Fig. 3D), and this phenomenon was reversed in Rescue and PV-DREADD groups ($p = 0.837$, Fig. 3D).

The number of errors per trial type and the number of trials needed to learn each rule are related, in that the more errors an animal makes, the more trials it will need. However, because the criterion is set at 8 consecutive correct responses, a few early errors would not affect the number of trials needed to learn the rule as much as errors later in the session would. Therefore, it is notable that the PV-DREADD group takes significantly more trials to learn the initial association ($p = 0.003$, Fig. 3E), but does not make significantly more errors (Fig. 3F, G). Interestingly, MK801-treated rats made significantly more perseverative errors compared to all other groups ($p < 0.001$ for all, Fig. 3G).

PV cell density, fluorescent intensity, and distance from the midline

To investigate the histological effects of MK801 treatment and PV-DREADD activation in greater detail, we examined multiple facets of PV staining in our 4 experimental groups after the animals completed the behavioral tests as shown in Fig. 1. Figure 4A–D shows sample images from the mPFC of Control, MK801, Rescue, and PV-DREADD group animals. When other parameters are carefully controlled, the fluorescent intensity is a reflection of PV protein expression levels. Nonetheless, there were no group differences in fluorescent level within the prelimbic (PL) or infralimbic (IL) mpFC subregions (Fig. 4E–H). However, in the PL, there was significant difference in the PV cell density across groups ($p = 0.027$). Specifically, the MK801 group had greater PV cell density than the Rescue group (MK801 vs Rescue: $p = 0.041$; MK801 vs PV-DREADD: $p = 0.069$, Fig. 4F). In the IL, there were no significant differences in cell density between groups ($p = 0.490$, Fig. 4I).

Measures of lateral distance are intended to give an impression of the relative changes in PV in superficial vs deep cortical layers. In the PL but not the IL, the Rescue group showed the highest average distance from the midline (Fig. 4G, J). Interestingly, a significant correlation was found between PV staining intensity in both PL and IL regions and rule shift trial performance. Specifically, animals with a higher average PV cell intensity required fewer trials to acquire the EDS (Fig. S4C, D), indicating the importance of prefrontal PV interneuron activity level for cognitive flexibility. In contrast, we found no correlations between T-maze performance and PV cell density, fluorescence intensity, or midline distance ($p > 0.05$ for all, Fig. S3). Likewise, there were also no correlations between set-shifting performance, neither rule shift trials nor perseverative errors, and PV cell density or midline distance ($p > 0.05$ for all, Figs. S4, S5).

DREADD-mediated activation of PV interneurons is effective in altering circuit-level inhibition

We next recorded sEPSCs and sIPSCs from the same pyramidal cells, which allowed for the calculation of a ratio between the amount of inhibitory and excitatory input the cells receive (Fig. 5A). Interestingly, there were significant group differences in sEPSC frequency ($F = 3.97$, $p < 0.05$; Fig. 5B) and sIPSC frequency ($F = 20.03$, $p < 0.0001$; Fig. 5C). However, no significant differences emerged when looking at sEPSC frequency in

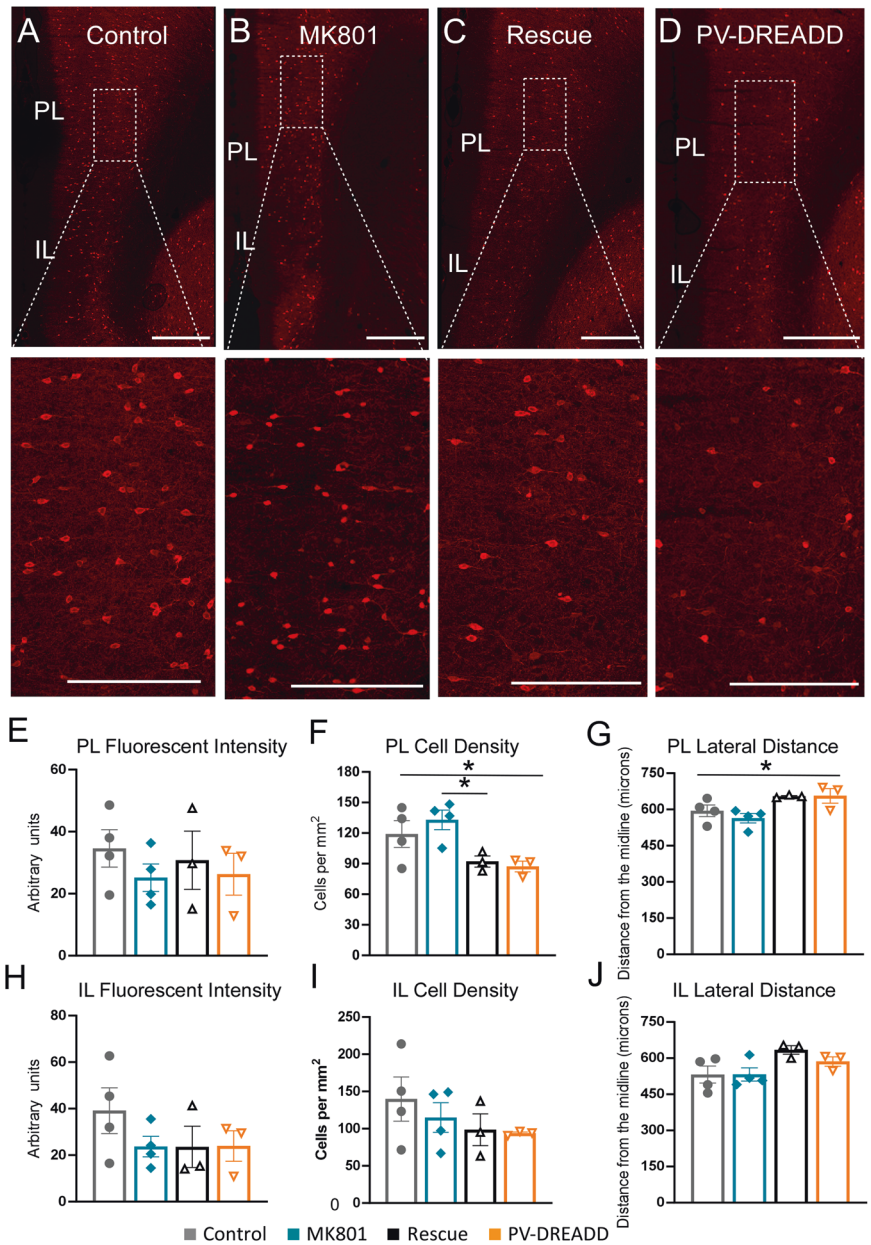


Fig. 4 Histological Results. A–D Sample images from animals used in behavioral experiments, immunostained for PV. **A** Sample image from a Control animal at 3.2 mm anterior from bregma. **B** Sample image from a MK801 animal at 2.7 mm. **C**, **D** Sample image from a Rescue and PV-DREADD group at 3.7 mm anterior to bregma. Top: scale bars are 500 μm. Bottom: scale bars are 250 μm. Rat Brain in Stereotaxic Coordinates by Paxinos and Watson, the 6th edition. **E**, **H** For fluorescent intensity, a two-way ANOVA showed no significant interaction between group and region ($p = 0.093$), nor a significant main effect of group ($p = 0.549$) or mPFC subregion ($p = 0.291$). **F**, **I** There was a significant difference in the PV density across the groups within the PL ($p = 0.027$; MK801 vs Rescue: $p = 0.041$) but not within the IL ($p > 0.05$). **G**, **J** A two-way ANOVA showed no significant interaction between group and mPFC subregion on PV cell distance from the midline ($p = 0.550$). However, a main effect of subregion ($p = 0.007$) and group ($p = 0{,}031$) was found. There was a significant group difference within the PL ($p = 0.035$) but not in the IL ($p > 0.05$). However, no pairwise comparisons were statistically significant.

comparison between different groups ($p > 0.05$) except Control vs. PV-DREADD ($p < 0.5$; Fig. 5B), nor in sIPSC frequency ($p > 0.05$ for all except Control vs. PV-DREADD, MK801 vs. PV-DREADD, and Rescure vs. PV-DREADD, $p < 0.0001$; Fig. 5C). There were also no differences among groups for both sEPSC and sIPSC amplitudes ($p > 0.05$; data not shown). Nevertheless, and importantly, we observed significant group differences in Layer II/III with regard to spontaneous E/I frequency ratio recorded from prefrontal pyramidal cells ($F = 11.47$, $p < 0.0001$; Fig. 5). When pairwise comparisons were performed, we saw an increased E/I ratio in MK801-treated animals compared to saline-treated animals ($p = 0.0001$). We also found that the Rescue group had a normalized E/I ratio (MK801 vs. Rescue: $p = 0.05$) and there was no difference between the Control and Rescue groups: $p > 0.05$). Finally, the PV-DREADD group also exhibited a robust reduction in E/I ratio compared to the MK801 group ($p < 0.001$). In addition, by examining the luteal and follicular phases of the rats, we found no correlation between the estrus cycle and the action potentials of pyramidal neurons in either layer II/III or layer V of the mPFC (Fig. S2).

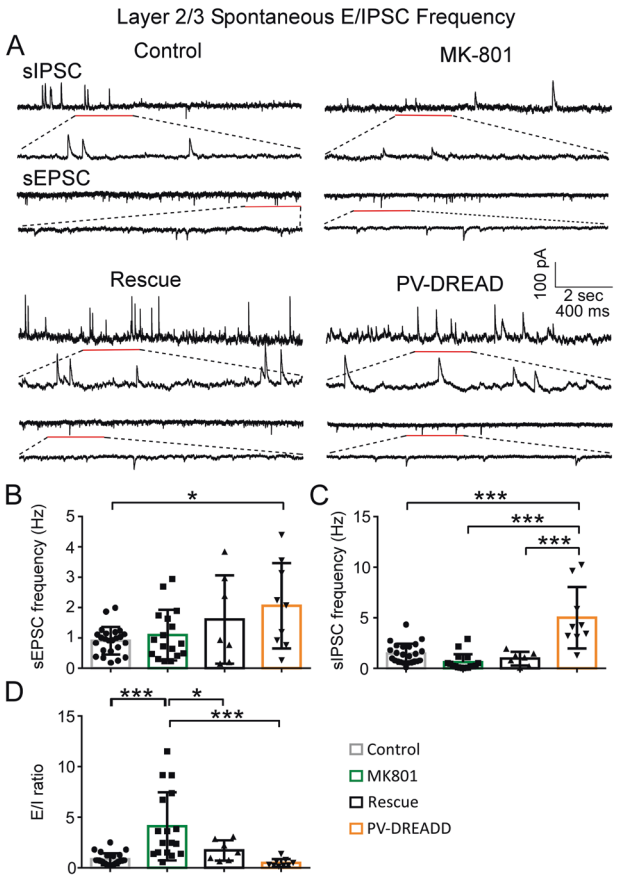


Fig. 5 Administration of MK801 increased the ratio of spontaneous E/IPSC frequency, which was rescued by activation of PV interneurons in the mPFC. A Sample spontaneous recordings from pyramidal cells in Layer II/III from each experimental group, top to bottom: Control, MK801, Rescue, and PV-DREADD. The upper pair sweeps of traces are sIPSCs, voltage-clamped at 0 mV with CPP, whereas the lower pair sweeps of traces are sEPSCs, voltage-clamped at 60 mV with CPP. In each pair, the upper sweep shows a longer segment, whereas the red bars with dashed lines in each pair are the enlargement of the segment. **B**–**D** The average event frequencies were measured from pyramidal cells in Layer II/III for each group. The average for excitatory events is shown in (**B**), that of inhibitory events is shown in (**C**), and the ratio is shown in (**D**). There were significant group differences in sEPSC frequency (**B**, $F = 3.97$, $p < 0.05$) and sIPSC frequency (**C**, $F = 20.03$, $p < 0.0001$). **B** There were no significant differences between different groups ($p > 0.05$) except Control vs. PV-DREADD ($p < 0.5$). **C** There were no differences in sIPSC frequency among the groups of Control, MK801, and Rescue ($p > 0.05$ for all) except Control vs. PV-DREADD, MK801 vs. PV-DREADD, and Rescure vs. PV-DREADD ($p < 0.0001$). **D** There was a significant group differences in in E/I frequency ratio ($F = 11.47$, $p < 0.0001$). Pairwise comparisons exhibited an increased E/I ratio in MK801-treated animals compared to Control animals ($p < 0.0001$). The increased E/I ratio was normalized by activated PV with excitatory DREADD (MK801 vs. Rescure: $p < 0.05$) while there was no difference between the Contorl and Rescue groups: $p > 0.05$). Finally, the PV-DREADD group also exhibited a robust reduction in E/I ratio compared to the MK801 group ($p < 0.0001$).

DISCUSSION

The pathophysiology underlying the cognitive symptoms of SZ is not well understood and no effective treatments exist. In this study, we explore the causal link between pathology in a specific subtype of GABAergic interneurons and cognitive deficits by using a novel pharmacogenetic method to regulate the functionality of these neurons for treatment of cognitive deficits. We found that pharmacogenetic activation of PV interneurons in the mPFC effectively rescued the cognitive deficits of MK801-treated rats. This study addresses the fundamental question of whether directly augmenting prefrontal inhibition is sufficient to ameliorate cognitive deficits in an animal model for SZ, potentially highlighting PV interneurons as therapeutic targets in clinical populations. Acute MK801 treatment has been shown to affect locomotion [24] and is often used to create hyperactivity, modeling the positive symptoms of SZ [24, 41]. However, given the time course of our MK801 treatment, acute effects on hyperactivity should no longer be present. Indeed, we found no change in locomotion, increasing the likelihood that the cognitive differences observed arose from distinct mechanisms.

We replicated the cognitive deficits associated with the MK801 model in both the T-maze and the set-shifting tasks [33, 42, 43]. Activation of the PV-DREADD in the prefrontal cortex of MK801-treated animals recovered performance for many of the measures collected in both paradigms. Learning and performing the T-maze delayed non-match to sample task requires working memory, spatial learning, and decision-making, all of which depend upon a well-functioning mPFC [33, 41]. MK801 induced significant deficits in performance at the 5-s and 60-s delays, but not at the 15-s and 30-s delay trials. Other network properties that are more important for success in intermediate delays may not significantly impacted by changes in PV cell activity. Increasing PV cell activity through DREADD activation was able to rescue the impairments at both shortest and longest delay. Interestingly, increasing PV cell activity above baseline did not significantly impact behavior overall, except in impairing performance on long delay (60 s) T-maze trials, consistent with our recent study [33].

In the set-shifting test of cognitive flexibility, it is striking that we found the most robust difference between groups in the number of perseverative errors made in the EDS. A perseverative response indicates that the animal is using the previously learned rule and has not adapted to the new rules in place [44, 45]. This type of cognitive inflexibility is characteristic of the deficits seen in SZ [46], and our rescue provided a significant improvement. Various imaging and lesion studies have demonstrated that distinct brain regions are important for the different types of rule shifts associated with this task. Lesions of the orbitofrontal cortex, a subregion of the PFC, in both rodent and primate studies, have been linked to deficits in reversal learning but not in the EDS phase of the task [47–55]. In contrast, lesions to the lateral or dorsolateral PFC (dlPFC) in humans and non-human primates [51–53, 56] and the mPFC in rats [45, 50] results in selectively impaired EDS performance, while leaving acquisition of the initial association and reversal learning intact.

Because we found no group differences in reversal learning, the orbitofrontal region seems to be less impacted by MK801 treatment. The intact acquisition of the initial association and the impairments specifically in EDS performance in our MK801 treated animals provide strong evidence for mPFC dysfunction in these animals. Injecting the PV-DREADD virus directly into the mPFC allowed for an effective rescue of the cognitive inflexibility induced by adolescent MK801 treatment. Given that our rescue provided a significant improvement, this further strengthens the rationale for targeting prefrontal inhibition via PV cells as a potential treatment for the cognitive deficits of SZ.

An altered E/I balance refers to a change in the possible network configurations at which the system may come into a new balance [57, 58]. Decreased inhibition may cause irrelevant information to not be properly suppressed and persist as "noise," resulting in a muddled representation of behaviorally relevant signals, and ultimately disrupted cognitive processes. We observed altered E/I balance in female MK801-treated rats in layer II/III but not layer V of the mPFC. A similar prefrontal E/I imbalance also occurs in layer V pyramidal cells in male rats that underwent adolescent but not adult MK801 exposure [40]. Human post-mortem studies provide some parallels with the laminar

difference in E/I ratio observed between female and male rats. In SZ, PV interneurons are most affected in layers III and IV [59–62]. In the dlPFC of SZ patients, a study found a 22% reduction of PV mRNA in layer III [63, 64]. The elevated E/I balance in layer II/III pyramidal cells of MK801-treated rats may reflect a similar layer-dependent PV cell disturbance, which would then be more responsive to the PV-DREADD intervention.

To target the observed PV disruptions, we activated prefrontal PV cells using an excitatory DREADDs driven by a PV promoter. Activation of the PV-DREADD increased the frequency of sIPSCs measured in neighboring pyramidal cells. We predicted that this increase in PV cell-driven inhibition would correct the E/I imbalances seen in the MK801-treated rats, thereby improving information processing and ultimately, cognition. In the set-shifting task, Rule Shift trials to criterion showed a robust deficit in adolescent MK801 animals and a near-complete restoration of function in the Rescue group. Therefore, we examined this aspect of cognitive performance in relation to PV cell distribution. We found that animals with a higher average PV cell fluorescent intensity required fewer trials to acquire the EDS. There was a significant correlation between PV cell fluorescent intensity and Rule Shift trials in both the PL and the IL. This finding underscores the importance of PV cells in the mPFC for maintaining cognitive flexibility, though it does not suggest independent roles for PV cells in the IL and PL for this task. This provides strong support for our hypothesis that the elevated E/I balance measured in the PFC of MK801-treated animals is attributable to changes in PV cells, and the activation of these cells is responsible for improved cognition in the Rescue group. Nonetheless, we previously reported that ~70% of neurons expressing the excitatory PV-DREADD used in this study exhibited a fast-spiking firing phenotype. Therefore, we cannot rule out that the improved cognition in the Rescue group could be due, in part, to activation of other interneuron types.

Our findings that PV cell activation can improve cognition in MK801-treated rats are consistent with several recent studies. Specifically, deficits in set shifting task were induced by inhibiting prefrontal interneurons in Dlx5/6 (+/−) mice [38], selectively inhibiting prefrontal PV interneurons in the prenatal maternal immune activation (MIA) mouse model [65], or disrupting normal patterns of activity in PV interneurons [66]. In contrast, ontogenetically stimulating PV interneurons rescued these deficits [38]. Chemogenetically activating PV interneurons in the hippocampus also restored cognition in a *LgDel*$^{+/-}$ genetic model of SZ [67, 68]. Enhancing mPFC PV interneuron activity in adulthood with a stabilized step-function opsin (SSFO) can also rescue behavioral deficits following developmental inhibition of mPFC PV interneurons [69]. Therefore, our work adds to the growing body of literature demonstrating a role for PV interneurons in cognition, and demonstrates that targeting these cells is a viable strategy for improving cognition in the adolescent MK-801 model.

Although this study provides new insight regarding the involvement of prefrontal PV cells in the neural circuitry and cognitive deficits associated with SZ, there are limitations. With the combination of an NMDA receptor-targeting pharmacological model and a PV cell activating excitatory DREADD, this study design cannot demonstrate that increasing PV cell activity is necessary for improving cognition, only that it is sufficient to improve cognition. Furthermore, our excitatory PV-DREADD did not target PV cells with 100% specificity. Future studies can expand on our conclusions by examining sex differences, involvement of other brain regions, additional details of prefrontal circuitry change, and alternative approaches to recapitulating the behavioral and physiological rescue produced by PV-DREADD activation.

The efficacy of our PV-DREADD to rescue cognitive performance in MK801-treated rats supports our hypothesis that increasing prefrontal PV cell activity may be a viable target for novel SZ treatments. The most pronounced electrophysiological finding was the elevated Layer II/III E/I balance in the adolescent MK801 animals and the subsequent return to baseline with PV-DREADD activation, providing further evidence for the theory of reduced prefrontal PV cell recruitment in the adolescent MK801 model. Combined with the behavioral effects, this suggests that a critical element of prefrontal circuitry for cognitive function is PV cell activity level. Reduced PV cell recruitment seems to be a point of convergence in the pathophysiology of SZ that may be remedied by directly targeting PV cells, regardless of the etiology of such deficits.

SZ is a complex disorder with multifactorial origins and heterogeneous presentations. However, we may come to appreciate how divergent causal factors ultimately converge on disruptions preferentially at prefrontal PV cells. This may be the fundamental pathology, leading to cognitive deficits through local changes in E/I balance, and more global downstream effects via disinhibited prefrontal projection neurons.

REFERENCES

1. Marder SR, Fenton W. Measurement and Treatment Research to Improve Cognition in Schizophrenia: NIMH MATRICS initiative to support the development of agents for improving cognition in schizophrenia. Schizophr Res. 2004;72:5–9.
2. Green MF, Harvey PD. Cognition in schizophrenia: Past, present, and future. Schizophr Res Cogn. 2014;1:e1–e9.
3. Allott K, Liu P, Proffitt TM, Killackey E. Cognition at illness onset as a predictor of later functional outcome in early psychosis: systematic review and methodological critique. Schizophr Res. 2011;125:221–35.
4. Bowie CR, Leung WW, Reichenberg A, McClure MM, Patterson TL, Heaton RK, et al. Predicting schizophrenia patients' real-world behavior with specific neuropsychological and functional capacity measures. Biol Psychiatry. 2008;63:505–11.
5. Benes FM, Berretta S. GABAergic interneurons: implications for understanding schizophrenia and bipolar disorder. Neuropsychopharmacol. 2001;25:1–27.
6. Lewis DA, Hashimoto T, Volk DW. Cortical inhibitory neurons and schizophrenia. Nat Rev Neurosci. 2005;6:312–24.
7. Curley AA, Arion D, Volk DW, Asafu-Adjei JK, Sampson AR, Fish KN, et al. Cortical deficits of glutamic acid decarboxylase 67 expression in schizophrenia: clinical, protein, and cell type-specific features. Am J Psychiatry. 2011;168:921–9.
8. Auger ML, Floresco SB. Prefrontal cortical GABA modulation of spatial reference and working memory. Int J Neuropsychopharmacol. 2015;18:pyu013.
9. Nakazawa K, Zsiros V, Jiang Z, Nakao K, Kolata S, Zhang S, et al. GABAergic interneuron origin of schizophrenia pathophysiology. Neuropharmacology. 2012;62:1574–83.
10. Lewis DA, Curley AA, Glausier JR, Volk DW. Cortical parvalbumin interneurons and cognitive dysfunction in schizophrenia. Trends Neurosci. 2012;35:57–67.
11. Gonzalez-Burgos G, Hashimoto T, Lewis DA. Alterations of cortical GABA neurons and network oscillations in schizophrenia. Curr Psychiatry Rep. 2010;12:335–44.
12. Uhlhaas PJ, Singer W. Neural synchrony in brain disorders: relevance for cognitive dysfunctions and pathophysiology. Neuron. 2006;52:155–68.
13. Lodge DJ, Behrens MM, Grace AA. A loss of parvalbumin-containing interneurons is associated with diminished oscillatory activity in an animal model of schizophrenia. J Neurosci. 2009;29:2344–54.
14. Lodge DJ, Grace AA. Gestational methylazoxymethanol acetate administration: a developmental disruption model of schizophrenia. Behav Brain Res. 2009;204:306–12.
15. Jeevakumar V, Driskill C, Paine A, Sobhanian M, Vakil H, Morris B, et al. Ketamine administration during the second postnatal week induces enduring schizophrenia-like behavioral symptoms and reduces parvalbumin expression in the medial prefrontal cortex of adult mice. Behav Brain Res. 2015;282:165–75.
16. Jeevakumar V, Kroener S. Ketamine administration during the second postnatal week alters synaptic properties of fast-spiking interneurons in the medial prefrontal cortex of adult mice. Cereb Cortex. 2015;26:1117–29.
17. Francois J, Ferrandon A, Koning E, Angst MJ, Sandner G, Nehlig A. Selective reorganization of GABAergic transmission in neonatal ventral hippocampal-lesioned rats. Int J Neuropsychopharmacol. 2009;12:1097–110.
18. Braun I, Genius J, Grunze H, Bender A, Moller HJ, Rujescu D. Alterations of hippocampal and prefrontal GABAergic interneurons in an animal model of psychosis induced by NMDA receptor antagonism. Schizophr Res. 2007;97:254–63.
19. Carlson GC, Talbot K, Halene TB, Gandal MJ, Kazi HA, Schlosser L, et al. Dysbindin-1 mutant mice implicate reduced fast-phasic inhibition as a final common disease mechanism in schizophrenia. Proc Natl Acad Sci USA. 2011;108:E962–70.

20. Fazzari P, Paternain AV, Valiente M, Pla R, Lujan R, Lloyd K, et al. Control of cortical GABA circuitry development by Nrg1 and ErbB4 signalling. Nature. 2010;464:1376–80.
21. Wen L, Lu Y-S, Zhu X-H, Li X-M, Woo R-S, Chen Y-J, et al. Neuregulin 1 regulates pyramidal neuron activity via ErbB4 in parvalbumin-positive interneurons. Proc Natl Acad Sci USA. 2020;107:1211–6.
22. Mei L, Xiong W-C. Neuregulin 1 in neural development, synaptic plasticity and schizophrenia. Nat Rev Neurosci. 2008;9:437–52.
23. Xi D, Keeler B, Zhang W, Houle JD, Gao WJ. NMDA receptor subunit expression in GABAergic interneurons in the prefrontal cortex: application of laser micro dissection technique. J Neurosci Meth. 2009;176:172–81.
24. Li Y-C, Snyder MA, Gao RY, Adelman AE, Zhang W. Group II metabotropic glutamate receptor agonist ameliorates MK-801-induced dysfunction of NMDA receptors via Akt/GSK-3beta pathway. Neuropsychopharmacol. 2011;36:1260–74.
25. Xi D, Zhang W, Wang HX, Stradtman GG, Gao WJ. Dizocilpine (MK-801) induces distinct changes of N-methyl-d-aspartic acid receptor subunits in parvalbumin-containing interneurons in young adult rat prefrontal cortex. Int J Neuropsychopharmacol. 2009;12:1395–408.
26. Wang HX, Gao WJ. Prolonged exposure to NMDAR antagonist induces cell-type specific changes of glutamatergic receptors in rat prefrontal cortex. Neuropharmacology. 2012;62:1808–22.
27. Thomases DR, Cass DK, Meyer JD, Caballero A, Tseng KY. Early adolescent MK-801 exposure impairs the maturation of ventral hippocampal control of basolateral amygdala drive in the adult prefrontal cortex. J Neurosci. 2014;34:9059–66.
28. Thomases DR, Cass DK, Tseng KY. Periadolescent exposure to the NMDA receptor antagonist MK-801 impairs the functional maturation of local GABAergic circuits in the adult prefrontal cortex. J Neurosci. 2013;33:26–34.
29. Dickerson J, Sharp FR. Atypical antipsychotics and a Src kinase inhibitor (PP1) prevent cortical injury produced by the psychomimetic, noncompetitive NMDA receptor antagonist MK-801. Neuropsychopharmacology. 2006;31:1420–30.
30. Farber NB, Wozniak DF, Price MT, Labruyere J, Huss J, St Peter H, et al. Age-specific neurotoxicity in the rat associated with NMDA receptor blockade: potential relevance to schizophrenia? Biol Psychiatry. 1995;38:788–96.
31. Olney JW, Labruyere J, Price MT. Pathological changes induced in cerebrocortical neurons by phencyclidine and related drugs. Science. 1989;244:1360–2.
32. Nathanson JL, Jappelli R, Scheeff ED, Manning G, Obata K, Brenner S, et al. Short promoters in viral vectors drive selective expression in mammalian inhibitory neurons, but do not restrict activity to specific inhibitory cell-types. Front Neural Circuits. 2009;3:19.
33. Ferguson BR, Gao WJ. Thalamic control of cognition and social behavior via regulation of gamma-aminobutyric acidergic signaling and excitation/inhibition balance in the medial prefrontal cortex. Biol Psychiatry. 2018;83:657–69.
34. Liu X-B, Jones EG. Localization of alpha type II calcium calmodulin-dependent protein kinase at glutamatergic but not gamma -aminobutyric acid (GABAergic) synapses in thalamus and cerebral cortex. Proc Natl Acad Sci USA. 1996;93:7332–6.
35. Paxinos G, Watson C. The Rat Brain in Stereotaxic Coordinates. 6th Edition, London Academic Press; 2006.
36. Gao WJ, Newman DE, Wormington AB, Pallas SL. Development of inhibitory circuitry in visual and auditory cortex of postnatal ferrets: immunocytochemical localization of GABAergic neurons. J Comp Neurol. 1999;409:261–73.
37. Gao WJ, Wormington AB, Newman DE, Pallas SL. Development of inhibitory circuitry in visual and auditory cortex of postnatal ferrets: immunocytochemical localization of calbindin- and parvalbumin-containing neurons. J Comp Neurol. 2000;422:140–57.
38. Cho KK, Hoch R, Lee AT, Patel T, Rubenstein JL, Sohal VS. Gamma rhythms link prefrontal interneuron dysfunction with cognitive inflexibility in Dlx5/6(+/−) mice. Neuron. 2015;85:1332–43.
39. Monaco SA, Matamoros AJ, Gao W-J. Conditional GSK3β deletion in parvalbumin-expressing interneurons potentiates excitatory synaptic function and learning in adult mice. Prog Neuropsychopharmacol Biol Psychiatry. 2020;100:109901.
40. Flores-Barrera E, Thomases DR, Tseng KY. MK-801 exposure during adolescence elicits enduring disruption of prefrontal E-I balance and its control of fear extinction behavior. J Neurosci. 2020;40:4881–7.
41. Li Y-C, Panikker P, Xing B, Yang S-S, Alexandropoulos C, McEachern EP, et al. Deletion of glycogen synthase kinase-3β in D2 receptor–positive neurons ameliorates cognitive impairment via NMDA receptor–dependent synaptic plasticity. Biol Psychiatry. 2021;87:745–55.
42. Tsukada H, Nishiyama S, Fukumoto D, Sato K, Kakiuchi T, Domino EF. Chronic NMDA antagonism impairs working memory, decreases extracellular dopamine, and increases D1 receptor binding in prefrontal cortex of conscious monkeys. Neuropsychopharmacology. 2005;30:1861–9.
43. Aultman JM, Moghaddam B. Distinct contributions of glutamate and dopamine receptors to temporal aspects of rodent working memory using a clinically relevant task. Psychopharmacol (Berl). 2001;153:353–64.
44. Barense MD, Fox MT, Baxter MG. Aged rats are impaired on an attentional set-shifting task sensitive to medial frontal cortex damage in young rats. Learn Mem. 2002;9:191–201.
45. Birrell JM, Brown VJ. Medial frontal cortex mediates perceptual attentional set shifting in the rat. J Neurosci. 2000;20:4320–4.
46. Crider A. Perseveration in schizophrenia. Schizophr Bull. 1997;23:63–74.
47. Jones B, Mishkin M. Limbic lesions and the problem of stimulus-reinforcement associations. Exp Neurol. 1972;36:362–77.
48. Eichenbaum H, Clegg RA, Feeley A. Reexamination of functional subdivisions of the rodent prefrontal cortex. Exp Neurol. 1983;79:434–51.
49. Meunier M, Bachevalier J, Mishkin M. Effects of orbital frontal and anterior cingulate lesions on object and spatial memory in rhesus monkeys. Neuropsychologia. 1997;35:999–1015.
50. Brown VJ, Bowman EM. Rodent models of prefrontal cortical function. Trends Neurosci. 2002;25:340–3.
51. Dias R, Robbins TW, Roberts AC. Primate analogue of the Wisconsin Card Sorting Test: effects of excitotoxic lesions of the prefrontal cortex in the marmoset. Behav Neurosci. 1996;110:872–86.
52. Dias R, Robbins TW, Roberts AC. Dissociation in prefrontal cortex of affective and attentional shifts. Nature. 1996;380:69–72.
53. Dias R, Robbins TW, Roberts AC. Dissociable forms of inhibitory control within prefrontal cortex with an analog of the Wisconsin Card Sort Test: restriction to novel situations and independence from "on-line" processing. J Neurosci. 1997;17:9285–97.
54. McAlonan K, Brown VJ. Orbital prefrontal cortex mediates reversal learning and not attentional set shifting in the rat. Behav Brain Res. 2003;146:97–103.
55. Chase EA, Tait DS, Brown VJ. Lesions of the orbital prefrontal cortex impair the formation of attentional set in rats. Eur J Neurosci. 2012;36:2368–75.
56. Owen AM, Roberts AC, Polkey CE, Sahakian BJ, Robbins TW. Extra-dimensional versus intra-dimensional set shifting performance following frontal lobe excisions, temporal lobe excisions or amygdalo-hippocampectomy in man. Neuropsychologia. 1991;29:993–1006.
57. Ferguson BR, Gao W-J. PV interneurons: critical regulators of E/I balance for prefrontal cortex-dependent behavior and psychiatric disorders. Front Neural Circuits. 2018;12:37.
58. Sohal VS, Rubenstein JLR. Excitation-inhibition balance as a framework for investigating mechanisms in neuropsychiatric disorders. Mol Psychiatry. 2019;24:1248–57.
59. Chung DW, Volk DW, Arion D, Zhang Y, Sampson AR, Lewis DA. Dysregulated ErbB4 Splicing in schizophrenia: selective effects on parvalbumin expression. Am J Psychiatry. 2016;173:60–8.
60. Hashimoto T, Volk DW, Eggan SM, Mirnics K, Pierri JN, Sun Z, et al. Gene expression deficits in a subclass of GABA neurons in the prefrontal cortex of subjects with schizophrenia. J Neurosci. 2003;23:6315–26.
61. Sakai T, Oshima A, Nozaki Y, Ida I, Haga C, Akiyama H, et al. Changes in density of calcium-binding-protein-immunoreactive GABAergic neurons in prefrontal cortex in schizophrenia and bipolar disorder. Neuropathology. 2008;28:143–50.
62. Tooney PA, Chahl LA. Neurons expressing calcium-binding proteins in the prefrontal cortex in schizophrenia. Prog Neuropsychopharmacol Biol Psychiatry. 2004;28:273–8.
63. Kaar SJ, Angelescu I, Marques TR, Howes OD. Pre-frontal parvalbumin interneurons in schizophrenia: a meta-analysis of post-mortem studies. J Neural Transm (Vienna). 2019;126:1637–51.
64. Enwright JF, Sanapala S, Foglio A, Berry R, Fish KN, Lewis DA. Reduced labeling of parvalbumin neurons and perineuronal nets in the dorsolateral prefrontal cortex of subjects with schizophrenia. Neuropsychopharmacology. 2016;41:2206–14.
65. Canetta S, Bolkan S, Padilla-Coreano N, Song LJ, Sahn R, Harrison NL, et al. Maternal immune activation leads to selective functional deficits in offspring parvalbumin interneurons. Mol Psychiatry. 2016;21:956–68.
66. Cho KKA, Davidson TJ, Bouvier G, Marshall JD, Schnitzer MJ, Sohal VS. Cross-hemispheric gamma synchrony between prefrontal parvalbumin interneurons supports behavioral adaptation during rule shift learning. Nat Neurosci. 2020;23:892–902.
67. Mukherjee A, Carvalho F, Eliez S, Caroni P. Long-lasting rescue of network and cognitive dysfunction in a genetic schizophrenia model. Cell. 2019;178:1387–1402.e14.
68. Marissal T, Salazar RF, Bertollini C, Mutel S, De Roo M, Rodriguez I, et al. Restoring wild-type-like CA1 network dynamics and behavior during adulthood in a mouse model of schizophrenia. Nat Neurosci. 2018;21:1412–20.
69. Canetta SE, Holt ES, Benoit LJ, Teboul E, Ogden RT, Harris AZ, et al. Mature parvalbumin interneuron function in prefrontal cortex requires activity during a postnatal sensitive period. eLife. 2022;11:80324.

ACKNOWLEDGEMENTS

We thank Theresa Connors for instruction in estrus cycle tracking and Andrew Gargiulo for help with the locomotion task.

AUTHOR CONTRIBUTIONS

LAC and WJG: conceived the project, designed the experiments, and wrote the manuscript. SSY: conducted physiological recording. LAC: conducted immunostaining, electrophysiological recording, surgery, and behavioral test, and analyzed the related data. EPM: behavioral tests (T-Maze and set-shifting). JTML: partial physiological recording. OWM: physiological data analysis. CAR: histological analysis. NRM: comments and manuscript editing and revision. BRF: conceived the project and manuscript editing.

FUNDING

These studies were funded by NIH R01MH085666, NIH R21MH111609, NARSAD Independent Award, Pennsylvania Commonwealth 4100072545 (CURE 2016), to W-JG, and The Helen S. Vernik SZ Pilot Research Project Grant through the Drexel Department of Psychiatry.

COMPETING INTERESTS

The authors declare no competing interests.

ADDITIONAL INFORMATION

Supplementary information The online version contains supplementary material available at https://doi.org/10.1038/s41386-023-01576-6.

Correspondence and requests for materials should be addressed to Brielle R. Ferguson or Wen-Jun Gao.

Reprints and permission information is available at http://www.nature.com/reprints

Publisher's note Springer Nature remains neutral with regard to jurisdictional claims in published maps and institutional affiliations.

Springer Nature or its licensor (e.g. a society or other partner) holds exclusive rights to this article under a publishing agreement with the author(s) or other rightsholder(s); author self-archiving of the accepted manuscript version of this article is solely governed by the terms of such publishing agreement and applicable law.